Exchange narrowing of magnetic resonance linewidths in inhomogeneous ferromagnets

V. A. Ignatchenko and V. A. Felk
L. V. Kirensky Institute of Physics SB RAS, 660036, Krasnoyarsk, Russia
(Received 19 October 2004; revised manuscript received 30 December 2004; published 21 March 2005)

The theory of exchange narrowing of ferromagnetic and spin-wave resonance linewidths in ferromagnets with the randomly inhomogeneous magnetic anisotropy is developed. The calculation is carried out by the method of averaged Green functions in the framework of the coherent potential approximation (CPA). One- and three-dimensional inhomogeneities with an arbitrary correlation wave number k_c are considered ($r_c=k_c^{-1}$ is the correlation radius of the inhomogeneities). The method of the approximate solution of the CPA equation is proposed which has the quick convergence. Effects of exchange narrowing of the magnetic resonance lines and shifts of these lines are calculated in the whole region of the values of the correlation wave number k_c. The approximate analytical expressions for the linewidth of the FMR in the limiting cases of the small and large k_c are obtained. Large narrowing of the FMR and spin-wave linewidths with the decrease of the correlation radius of inhomogeneities is the substantiation of the main advantage of nanocrystalline and amorphous materials over usual polycrystals when they are used at high frequency devices.

DOI: 10.1103/PhysRevB.71.094417 PACS number(s): 75.30.Ds, 76.50.+g

I. INTRODUCTION

It is well known that inhomogeneities of the internal magnetic field in a matter caused by different physical reasons lead to broadening of the magnetic resonance line. For example, it can be magnetodipole fields of impurity ions in paramagnets. Fields of the magnetic anisotropy, the direction of which is different in the different grains, leads to this effect in ferromagnetic polycrystals. The linewidth ΔH resulting from this phenomenon has an order of value of the rms fluctuations of the internal fields for the noninteracting inhomogeneities. In the case of the polycrystal this simplest picture corresponds to the situation when the value of grains D_0 much more then the length of exchange correlations that have the order of thickness of a domain wall, $L_0=(A/K)^{1/2}$, where A and K are the exchange and anisotropy parameters, respectively. In this case oscillations of the magnetic moment in different grains can be considered as independent (the independent grains approximation) and their resonance frequencies (or resonance fields) are determined by the value of the anisotropy and the direction of the axis in each crystalline. This situation has been considered in the classic papers by Schlomann[1,2] (see, also Ref. 3). A shape of the resonance line for a polycrystal in this case can be found by the simple averaging of the expression for the shape of the line in the one grain with the corresponding distribution function of direction of the anisotropy axes. Under the condition of the uniform distribution of the anisotropy axes the rms fluctuation of the anisotropy field and, correspondingly, the resonance linewidth is of the order of a value of the anisotropy field, $\Delta H_0 \approx (5/3)H_a$, where $H_a=2K/M$, M is the magnetization. It must be emphasized that this linewidth has no relation to any relaxation processes in the system. The latter determine the linewidth in each crystalline which can be much less than ΔH_0. The situation is sharply complicated for the media where oscillations of the spins, situated in different internal fields, are bound by the exchange interaction. Effects of this interaction develop themselves in narrowing of the magnetic resonance line from the initially widest line corresponding to the independent inhomogeneities. The theory of such exchange narrowing of the electron paramagnetic resonance (EPR) and nuclear magnetic resonance (NMR) lines is well developed for the paramagnetic systems.[4–6] For the magneto-ordered media the consistent theory of exchange narrowing of the resonance line is absent. Meanwhile the most perspective magnetic materials, nanocrystalline, and amorphous alloys, belong to the media with the exchange-bound inhomogeneities. Approximate approaches which have been developed earlier for taking into account exchange as well as magnetodipole narrowing of the ferromagnetic resonance (FMR) line[1,2,7,8] do not describe experimental results at these types of media.

Because of this, Rubinstein, Harris, and Lubitz[9] for the explanation of their experiments, extended to the region of the FMR the scaling arguments that were initially developed in Refs. 10–12 (see also a review[13]) for describing the processes of the quasistatical remagnetizations and for calculating the hysteresis loops and coercive fields of nanocrystalline magnetic materials. We recollect first how these arguments look for the hysteresis loop. If $L_0 \ll D_0$ and the independent grains approximation is valid the hysteresis loop of a polycrystal can be calculated accordingly to the classic paper by Stoner and Wohlfart,[14] by the direct averaging of the hysteresis loops of individual grains with the corresponding distribution function of the anisotropy axes of these grains. When the opposite condition, $L_0 \gg D_0$, is valid the whole volume of the sample breaks up on stochastic domains with a random orientation of the magnetization; the average dimension of the domain L must be calculated self-consistently. A large number of the grains, $N=(L/D_0)^d$, where d is the dimensionality of the inhomogeneities, are thrown into the volume of each stochastic domain. The magnetization of each such domain moves as a single whole in the field of the effective anisotropy $\overline{K}$ which has the order of a value of the rms fluctuation of the crystalline magnetic anisotropy in the volume of the each domain, $\overline{K}=K/N^{1/2}=K(L/D_0)^{d/2}$. The magnetiza-

tions of different domains weakly interact with each other and, in the first approximation, these stochastic domains can be considered as independent. Thus, we can again use the Stoner and Wohlfart method of direct averaging for calculating of the hysteresis loop, however apply it now to the stochastic domains with the effective anisotropy $\overline{K} \ll K$ and dimension $L \gg D_0$ but not for the grains. As a result the hysteresis loop of the nanocrystal will be obtained with taking account of its exchange narrowing in comparison with the maximum broad loop corresponding to the usual polycrystal. The following scaling arguments are used for obtaining the equation for $\overline{K}$. The average dimension of the stochastic domain equal to the length of the exchange correlations not in the medium with the anisotropy K but in the medium with the unknown anisotropy $\overline{K}$, that is $L=(A/\overline{K})^{1/2}$. Substituting this L in the expression for $\overline{K}$, which is shown above, one can obtain the equation for $\overline{K}$. The next formula follows from this equation:

$$\overline{K}/K = a\left(\frac{bD_0}{L_0}\right)^{2d(4-d)}, \tag{1}$$

where a and b are unknown constants of the order of the unit.

As the coercitive force H_c is proportional to the anisotropy field of the stochastic domains $\overline{H_a}=2\overline{K}/A$, the next relationship follows for the three-dimensional inhomogeneities from Eq. (1), $H_c \propto D_0^6$. This dependency was observed repeatedly[11,13] at the some interval of the grains dimension D_0.

The authors of Ref. 9 made their proposal that analogous arguments can be used also for the estimation of exchange narrowing of the FMR line in nanocrystals. If for calculating the FMR linewidth in the case $L_0 \ll D_0$ the Schlomann's method[1] of the direct averaging over the independent grains is valid, that in the opposite case $L_0 \gg D_0$ one can again apply this method but to the independent stochastic domains. If the FMR linewidth ΔH_0 is proportional to the anisotropy K in the first case, it will be narrowed by the exchange interaction in the second case,

$$\Delta H/\Delta H_0 = \overline{K}/K, \tag{2}$$

where $\overline{K}$ is determined by Eq. (1).

The experiments were carried out in Ref. 9 in which the dimension of the grains D_0 as well as the FMR linewidth ΔH increase simultaneously in several times in the process of annealing the sample. It confirms that the scaling arguments play one of the main roles in the physical mechanism leading not only to exchange narrowing of the hysteresis loops but also to exchange narrowing of the FMR linewidth in nanocrystals (and also, in amorphous alloys where the correlation length of fluctuations of the local magnetic anisotropy axis $2r_c$ plays the role of the grain dimension D_0 in the nanocrystals).

However, the transfer of the scaling arguments to the region of the FMR does not take into account, at least, two essential factors. First, the length of the exchange correlations L becomes a function of the magnetic field in the fields $H \gtrsim H_a$ which are characteristic for the FMR region.[15] Second, and this is the main factor, this approach does not take into account the contribution of the processes of spin-wave scattering from the inhomogeneities of the anisotropy in the linewidth. These processes are especially essential for the spin-wave resonances. It has been shown in Ref. 15 that the damping ω'', which is due to these processes, increases ($\omega'' \propto k$) at $k \ll k_c$ and decreases ($\omega'' \propto k^{-1}$) at $k \gg k_c$ with the increase of the wave number k (here $k_c = r_c^{-1}$ is the correlation wave number of the inhomogeneities). In Ref. 15 as well as in following papers[16–18] the calculation of eigenfrequencies and dampings of spin waves carried out in the first approximation of the perturbation theory over the rms fluctuations of the inhomogeneities parameter. That approximation did not take into account the effects of inhomogeneous fields leading to the nonrelaxation contributions into the linewidth, the dependence of which on the exchange correlations were discussed above in the framework of the scaling arguments. On the other hand, the scaling arguments do not take into consideration the contribution of the relaxation processes to the magnetic resonance linewidth. To take into account both these effects and develop the consequent theory of exchange narrowing of magnetic resonance lines in magneto-ordered media, the taking account of the multiple scattering of the waves from inhomogeneities described by the corresponding Green function is required.

The objective of this paper is the calculation of the shapes and widths of the FMR and spin-wave resonance lines with taking into consideration the multiple scattering processes of spin waves on the one-dimensional (1D) and three-dimensional inhomogeneities of the magnetic anisotropy by the method of the averaged Green function in the coherent potential approximation (CPA) in the whole diapason of the relationship between L_0 and D_0 from $D_0 \ll L_0$ (the limit of independent grains) to $L_0 \gg D_0$ (the limit of strongly coupled grains).

Different physical effects make a contribution to the local magnetic anisotropy in the modern nanocrystalline and amorphous alloys: the local crystalline anisotropy, anisotropy of internal random elastic strains, anisotropy of grain shapes, and so on. Such effective local anisotropy is inhomogeneous for both the value of the anisotropy and direction of its axis. However, the theoretical description of the spin wave spectrum modification, which is caused by these two types of inhomogeneities of the anisotropy, leads to the problems of the essentially different difficulties. The matter is that when only the value of the magnetic anisotropy fluctuates, the only spin waves become random functions but the ground magnetic state remains uniform. But when the direction of the magnetic anisotropy axis fluctuates the ground state becomes inhomogeneous, the statical stochastic magnetic structure (SMS) appears to also interact with the spin waves.[15,19] Therefore, in the latter case there are two canals of the acting of the anisotropy inhomogeneities on the spin waves, direct and through the SMS. This leads to the sharp complication of the mathematical problem. However, the second canal can be suppressed in the magnetic fields $H \gg H_a$ because the rms fluctuations of the SMS decrease with the increase of H. The situation when $H \gg H_a$ is characteristic in many cases for the FMR and spin-wave resonance experiments. That is why we

neglect the effect associated with the SMS. This permits us to consider the model which under the correspondent redefinitions of the parameters describes the influence of the inhomogeneities of the magnetic anisotropy value (correctly) as well as the inhomogeneities of the magnetic anisotropy axis direction (in the approximation $H \gg H_a$).

II. MODEL AND METHOD

We describe the dynamics of ferromagnetic medium by the classic Landau-Lifshitz equation

$$\dot{\mathbf{M}} = -g \cdot [\mathbf{M} \times \mathbf{H}_{\text{eff}}], \tag{3}$$

where $\mathbf{M}$ is the magnetization, g is the gyromagnetic ratio, and $\mathbf{H}_{\text{eff}}$ is the effective magnetic field which is determined by the expression

$$\mathbf{H}_{\text{eff}} = -\frac{\partial \mathcal{H}}{\partial \mathbf{M}} + \frac{\partial}{\partial \mathbf{x}} \frac{\partial \mathcal{H}}{\partial (\partial \mathbf{M}/\partial \mathbf{x})}. \tag{4}$$

We choose the energy density $\mathcal{H}$ in the form

$$\mathcal{H} = \frac{1}{2} \cdot \alpha \left(\frac{\partial \mathbf{M}}{\partial \mathbf{x}} \right)^2 - \frac{1}{2} \cdot \beta(\mathbf{x}) [\mathbf{M}\mathbf{l}(\mathbf{x})]^2 - \mathbf{M}\mathbf{H} - \frac{1}{2} \cdot \mathbf{M}\mathbf{H}_m, \tag{5}$$

where $\alpha = 2A/M^2$ is the exchange parameter, $\beta(\mathbf{x})$ and $\mathbf{l}(\mathbf{x})$ are the value of the magnetic anisotropy and direction of its axis, respectively, $\mathbf{H}$ is the external magnetic field, $\mathbf{H}_m$ is the magnetodipole field, and $\mathbf{x} = (x, y, z)$.

At first we consider the model in which the only value of the magnetic anisotropy is inhomogeneous, while the direction of the anisotropy axis $\mathbf{l}$ is uniform and coincides with the direction of the magnetic field $\mathbf{H}$ which is parallel to the z axis. We represent the value of the anisotropy in the form

$$\beta(\mathbf{x}) = \beta[1 + \gamma\rho(\mathbf{x})], \tag{6}$$

where β is the average value of the anisotropy, γ is its relative rms fluctuations, and $\rho(\mathbf{x})$ is a centered ($\langle \rho \rangle = 0$) and normalized ($\langle \rho^2 \rangle = 1$) random function of coordinates. The angle brackets here and farther denote averaging over the ensemble of random realizations. Stochastic properties of the function $\rho(\mathbf{x})$ are characterized by a correlation function depending on the difference of the coordinates $\mathbf{r} = \mathbf{x} - \mathbf{x}'$,

$$K(\mathbf{r}) = \langle \rho(\mathbf{x}) \rho(\mathbf{x} + \mathbf{r}) \rangle, \tag{7}$$

or by the spectral density $S(\mathbf{k})$ which is connected with $K(\mathbf{r})$ by a Fourier transformation

$$S(\mathbf{k}) = \frac{1}{(2\pi)^3} \int K(\mathbf{r}) e^{-i\mathbf{k}\mathbf{r}} d\mathbf{r}. \tag{8}$$

We perform the usual linearization of Eq. (1) ($M_z \approx M; M_x, M_y \ll M$), take $M_x, M_y \propto e^{i\omega t}$, and introduce the circular projections

$$m^{\pm} = M_x \pm i M_y. \tag{9}$$

We assume that the sample has symmetrical shape in the xy plane. In this case the equations for $m^{\pm}$ get uncoupled and for the resonance projection m^+ we have the equation

$$\nabla^2 m^+ + [\nu - \eta\rho(\mathbf{x})] m^+ = 0, \tag{10}$$

where the notations are introduced

$$\nu = \frac{\omega - \omega_0}{\alpha g M}, \quad \eta = \frac{\gamma\beta}{\alpha}. \tag{11}$$

Here ω_0 is the uniform FMR frequency

$$\omega_0 = g[H - (N_z - N_{xy})M - H_a], \tag{12}$$

where N_z and N_{xy} are the demagnetization factors along the z axis and in the xy plane, respectively, and $H_a = \beta M$ is the average value of the anisotropy field.

Note, that the wave equation for electromagnetic or elastic waves in the scalar approximation also has the form of Eq. (10) with corresponding redefinitions of the parameters. So simple a form of the equation for the spin waves is a consequence of the cylindrical symmetry of the problem with respect to the z axis. For the problem with the inhomogeneous direction of the anisotropy axis $\mathbf{l} = \mathbf{l}(\mathbf{x})$ this symmetry disappears and the equations for the projections m^+ and m^- become coupled. Besides that, the inhomogeneity of the anisotropy direction leads to the inhomogeneity of the magnetization ground state, the SMS structure with the components $M_x(\mathbf{x})$ and $M_y(\mathbf{x})$ appears. This in turn leads to the appearance of new terms in the equations for the spin waves which describe the interaction of the projections $m^{\pm}$ with the components of the SMS. As a result, the mathematical problem dramatically complicates.[15] If we neglect the coupling of m^+ with the nonresonance projection m^- and with SMS components, the only terms will be saved which describe the direct interaction of m^+ with the random functions l_x^2, l_y^2, and l_z^2, where l_i are the projections of the vector $\mathbf{l}$ on the coordinate axes. It is easy to show that the equation for m^+ in this case has the form of Eq. (10) in which the parameters η and ω_0 for the case of the uniform distribution of the anisotropy axis in all directions have the forms

$$\eta = \frac{\beta}{\sqrt{5}\alpha} = \frac{1}{\sqrt{5}} \frac{H_a}{\alpha M},$$

$$\omega_0 = g[H - (N_z - N_{xy})M]. \tag{13}$$

In distinction to Eq. (12) the term H_a is absent now in the equation for ω_0 because the averaged anisotropy field is equal to zero in this case. So, solving the equation (10) we shall simultaneously investigate the correct model of the value of the magnetic anisotropy fluctuations and the approximate model of the anisotropy axis direction fluctuations.

Introducing the Green function $G(\mathbf{x}, \mathbf{x}_0)$ we rewrite Eq. (10) in the form

$$\nabla^2 G(\mathbf{x}, \mathbf{x}_0) + [\nu - \eta\rho(\mathbf{x})] G(\mathbf{x}, \mathbf{x}_0) = (2\pi)^3 \delta(\mathbf{x} - \mathbf{x}_0). \tag{14}$$

The numerical coefficient $(2\pi)^3$ is introduced on the right-hand side of this equation for the simplification of the following equations. In the uniformly random media, where all

variables depend only on the difference of the coordinates $\mathbf{r}=\mathbf{x}-\mathbf{x}'$, the Dyson equation for the averaged Green function has the form (see, for example, Ref. 20):

$$\overline{G}(\mathbf{x}-\mathbf{x}_0) = G_0(\mathbf{x}-\mathbf{x}_0) + \int\int G_0(\mathbf{x}-\mathbf{x}_1)Q(\mathbf{x}_1-\mathbf{x}_2) \times \overline{G}(\mathbf{x}_2-\mathbf{x}_0)d\mathbf{x}_1 d\mathbf{x}_2, \quad (15)$$

where $\overline{G}(\mathbf{r})$ is the averaged Green function, $G_0(\mathbf{r})$ is the initial Green function for the uniform media, $Q(\mathbf{r})$ is the mass operator which depends on the correlation function $K(\mathbf{r})$ as well as on $G_0(\mathbf{r})$. Representing these functions in the form of the Fourier integrals

$$\overline{G}(\mathbf{r}) = \int \overline{G}(\mathbf{k})e^{i\mathbf{kr}}d\mathbf{k},$$

$$G_0(\mathbf{r}) = \int G_0(\mathbf{k})e^{i\mathbf{kr}}d\mathbf{k}, \quad Q(\mathbf{r}) = \int M(\mathbf{k})e^{i\mathbf{kr}}d\mathbf{k}, \quad (16)$$

we obtain the Dyson equation for the Fourier transformations $\overline{G}(\mathbf{k})$, $G_0(\mathbf{k})$, and $M(\mathbf{k})$ and find $\overline{G}(\mathbf{k})$ from

$$\overline{G}(\mathbf{k}) = \frac{1}{G_0^{-1}(\mathbf{k}) - M(\mathbf{k})}. \quad (17)$$

For the case of the infinitive medium $G_0^{-1}=\nu-k^2$ and Eq. (17) takes the form

$$\overline{G}(\mathbf{k}) = \frac{1}{\nu - k^2 - M(\mathbf{k})}. \quad (18)$$

Here $M(\mathbf{k})$ is the infinite power series in the Fourier transformations of the Green functions $G_0(\mathbf{k})$ and the spectral densities $S(\mathbf{k})$. The modern methods of summation of this series[21–23] are based on the developing and approximate solution of the self-consistent equation for $M(\mathbf{k})$.

A much used method of obtaining the self-consistent equation for the mass operator $M(\mathbf{k})$ is the method of the CPA. After the first derives of the CPA equation in Refs. 24 and 25 a number of other variants of the derives, extensions, and development were suggested in original papers[26,27] as well as in reviews[28] and books[21–23].

We present here one more simple derive. Changing $\mathbf{k}$ by $\mathbf{k}_1$ in Eq. (18), multiplying this equation by $\eta^2 S(\mathbf{k}-\mathbf{k}_1)$, and integrating it over $\mathbf{k}_1$ we obtain

$$\eta^2 \int \overline{G}(\mathbf{k}_1)S(\mathbf{k}-\mathbf{k}_1)d\mathbf{k}_1 = \eta^2 \int \frac{S(\mathbf{k}-\mathbf{k}_1)d\mathbf{k}_1}{\nu - k_1^2 - M(\mathbf{k}_1)}. \quad (19)$$

For obtaining the self-consistent equation for $\mathbf{M}(\mathbf{k})$ we require that the left-hand side of Eq. (19) is approximately equal to $\mathbf{M}(\mathbf{k})$:

$$M(\mathbf{k}) \approx \eta^2 \int \overline{G}(\mathbf{k}_1)S(\mathbf{k}-\mathbf{k}_1)d\mathbf{k}_1. \quad (20)$$

Carrying out the inverse Fourier transformation we obtain that this requirement corresponds to the fulfillment of the following approximate equality:

$$\begin{aligned} Q(\mathbf{x}-\mathbf{x}_0) &\approx \eta^2 \overline{G}(\mathbf{x}-\mathbf{x}_0)K(\mathbf{x}-\mathbf{x}_0) \\ &= \eta^2 G_0(\mathbf{x}-\mathbf{x}_0)K(\mathbf{x}-\mathbf{x}_0) + \eta^4 \int\int G_0(\mathbf{x}-\mathbf{x}_1)G_0(\mathbf{x}_1-\mathbf{x}_2)G_0(\mathbf{x}_2-\mathbf{x}_0)K(\mathbf{x}_1-\mathbf{x}_2)K(\mathbf{x}-\mathbf{x}_0)d\mathbf{x}_1 d\mathbf{x}_2 \\ &+ \eta^6 \int\int\int\int G_0(\mathbf{x}-\mathbf{x}_1)G_0(\mathbf{x}_1-\mathbf{x}_2)G_0(\mathbf{x}_2-\mathbf{x}_3)G_0(\mathbf{x}_3-\mathbf{x}_4)G_0(\mathbf{x}_4-\mathbf{x}_0)[K(\mathbf{x}_1-\mathbf{x}_2)K(\mathbf{x}_3-\mathbf{x}_4) \\ &+ K(\mathbf{x}_1-\mathbf{x}_3)K(\mathbf{x}_2-\mathbf{x}_4) + K(\mathbf{x}_1-\mathbf{x}_4)K(\mathbf{x}_2-\mathbf{x}_3)]K(\mathbf{x}-\mathbf{x}_0)d\mathbf{x}_1 d\mathbf{x}_2 d\mathbf{x}_3 d\mathbf{x}_4 + \cdots . \end{aligned} \quad (21)$$

It follows from Eq. (21) that the left-hand side of the exact equation (19) takes into account only those diagrams that have correlations between the initial point $\mathbf{x}_0$ and final point $\mathbf{x}$. Comparing Eq. (21) with the rigorous representation of the mass operator $Q(\mathbf{r})$ in the form of series in the correlators[20] one can see that the formula (21) is exact in the first order of $K(\mathbf{r})$, takes into account one diagram from two in the second order, three diagrams from 10 in the third order, and so on. This is a drawback of the CPA method. However, a large body of comparisons of the results obtained by the CPA method with the direct numerical modeling (for the density of states see, for example, Ref. 23) show that this drawback is essentially overcome by the main advantage of this method permeating to make the analytical summation (that is, to reduce to an integral equation) of considering in its framework diagrams all orders for the mass operator of the Green function. It is convenient to introduce the mass term $M_{\mathbf{k}}=M(\mathbf{k})$ and to rewrite the basic system of the CPA equations (18) and (19) in the form

$$\overline{G}_k = \frac{1}{\nu - k^2 - M_k}, \quad (22)$$

$$M_k = \eta^2 \int \frac{S(\mathbf{k}-\mathbf{k}_1)d\mathbf{k}_1}{\nu - k_1^2 - M_{k_1}}. \quad (23)$$

III. ANALYSIS OF SOLUTIONS OF THE CPA EQUATIONS

We model the correlation properties of inhomogeneities by the exponential function $K(\mathbf{r})$ and the corresponding spectral density $S(\mathbf{k})$. For the 1D and 3D inhomogeneities these functions have the form, respectively,

$$\text{1D}, \quad K(r_z) = e^{-k_c|r_z|}, \quad S(k) = \frac{1}{\pi}\frac{k_c}{k_c^2 + k^2}, \tag{24}$$

$$\text{3D}, \quad K(r) = e^{-k_c r}, \quad S(k) = \frac{1}{\pi^2}\frac{k_c}{(k_c^2 + k^2)^2}. \tag{25}$$

Here k_c is the correlation wave number of the inhomogeneities ($r_c = k_c^{-1}$ is the correlation radius; for the case of poly- or nanocrystal $2r_c$ is equal to the size of the grain D_0).

A. Method of chain fractions

The integral equation (23) cannot be solved exactly for even such simple functions as Eqs. (24) and (25). One way of an approximate analysis of this equation is representing it in the form of the infinite chain fractions of the integral expressions which are proportional to η^2,

$$M_{\mathbf{k}} \approx \int \frac{\eta^2 S(\mathbf{k}-\mathbf{k}_1)d\mathbf{k}_1}{\nu - k_1^2 - \eta^2 \int \dfrac{S(\mathbf{k}_1-\mathbf{k}_2)d\mathbf{k}_2}{\nu - k_2^2 - \eta^2 \int \dfrac{S(\mathbf{k}_2-\mathbf{k}_3)d\mathbf{k}_3}{\nu - k_3^2 - \eta^2 \int \cdots}}}. \tag{26}$$

Restricting in this formula to the first link of the chain fractions which is proportional to η^2 we obtain M_k in the Bourret approximation[20,29]

$$M_{\mathbf{k}} = \eta^2 \int \frac{S(\mathbf{k}-\mathbf{k}_1)d\mathbf{k}_1}{\nu - k_1^2}. \tag{27}$$

Substituting $S(\mathbf{k})$ in the form of Eqs. (24) or (25) in Eq. (27) and performing the integration with the help of the residue theory we obtain for the 1D and 3D inhomogeneities, respectively,

$$\text{1D}, \quad M_k = \frac{\eta^2}{(\sqrt{\nu} - ik_c)^2 - k^2}\left(1 - \frac{ik_c}{\sqrt{\nu}}\right), \tag{28}$$

$$\text{3D}, \quad M_k = \frac{\eta^2}{(\sqrt{\nu} - ik_c)^2 - k^2}. \tag{29}$$

Substituting these expressions in Eq. (22) we obtain that in this approximation the imaginary part of the Green function G'' as a function of the frequency ν and correlation wave number k_c for the 1D inhomogeneities has the shape that is shown in Fig. 1. The Green function is normalized on the value $G''_m = 1/\eta$ in this figure. The form of the Green function for the 3D inhomogeneities under the condition $k_c/\sqrt{\nu} \ll 1$ differs little from Fig. 1. The appearance of two resonance peaks in the curve $G''(\nu)$ at the small values of k_c has no physical sense and is a result of using the Bourret approximation. The widths of these peaks are proportional to the damping that is due to the scattering of the spin waves by the inhomogeneities. They are determined by the expression

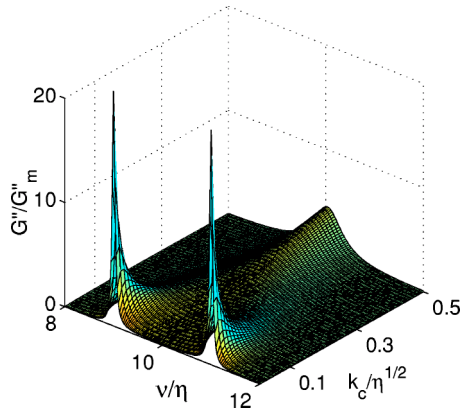

FIG. 1. The dependence of the imaginary part of the Green function G'' on the normalized frequency ν/η for different values of the normalized correlation wave number of the 1D inhomogeneities $k_c/\sqrt{\eta}$ in the approximation of the only one link of the chain fraction Eq. (26) (Bourret approximation). The minimum value of $k_c/\sqrt{\eta}$ corresponds to 0.7×10^{-2}.

$$\Delta\nu \approx 2k_c\sqrt{\nu}. \tag{30}$$

The distance between these peaks, as it will be shown below, from taking into account the following approximations, is approximately equal of the resonance linewidth that is due not to the damping but to the stochastic spread in values of the frequencies. With the increase of k_c the distance between them decreases, and two peaks merge all together under the condition

$$k_c^2\nu \geqslant \eta^2. \tag{31}$$

The Bourret approximation is valid at least qualitatively only in the region of the existence of the one resonance maximum in the function $G''(\nu)$.

Taking into account in Eq. (26) two integral terms and performing integration with respect to k_2 we obtain the next approximation for M_k for the 1D inhomogeneities,

$$M_k = \eta^2 \int \frac{S(k-k_1)dk_1}{\nu - k_1^2 - \dfrac{\eta^2}{(\nu - ik_c)^2 - k_1^2}\left(1 - \dfrac{ik_c}{\sqrt{\nu}}\right)}. \tag{32}$$

The integral in Eq. (32) was performed with the help of the residue theory exactly because a biquadratic form in k_1 can be obtain in its denominator. A cumbrous expression has been obtained that we do not present here. The dependence of $G''(\nu)$, calculated with the help of this expression for M_k, is shown in Fig. 2 by circles. In this approximation the function $G''(r)$ has three resonance peaks at the small values of k_c; the region of the existence of the single-mode solution spreads in the direction of smaller k_c compared with those which are determined by Eq. (31) for the Bourret approximation. The next approximations which take into account greater numbers of the links of the chain fraction Eq. (26) are

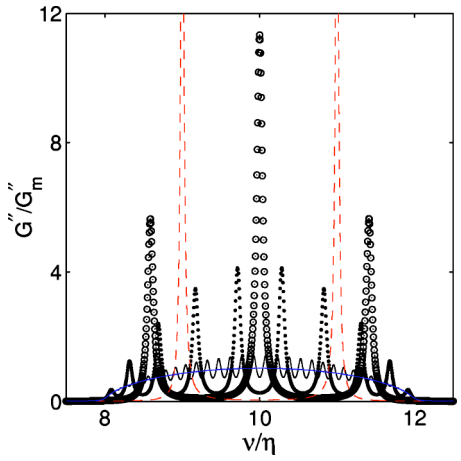

FIG. 2. The dependence of G'' on the normalized frequency ν/η at $k_c/\eta=0.7\times10^{-2}$ for different numbers n of the links of the chain fraction Eq. (26): $n=1$, dashed, two-modes curve; $n=2$, circles, three-modes curve; $n=9$, dots, 10-modes curve; $n=40$, solid 41-modes curve; the solid single-mode curve with the amplitude $G''/G_m=1$ corresponds to the limiting case $n\to\infty$.

obtained by the numerical integration. In Fig. 2 the dependencies $G''(\nu)$ are depicted for different numbers n of the links of the fraction Eq. (26). It is seen that the curve with $n+1$ peaks corresponds to the nth approximation. The square under each curve remains constant, that is why the amplitudes of the peaks decrease with the increase of the number of the peaks. The convergence of the approximate solutions to the limiting single-mode curve with the increase of the number of approximation n for small values of k_c goes on very slowly and becomes worse with the decrease of k_c. As is seen from Fig. 2 at $k_c/\sqrt{\eta}\sim10^{-2}$ that even taking into account the 40 links of the fraction and, correspondingly, performing the 40 successive numerical integrations does not lead to the single-mode function $G''(\nu)$. The limiting single-mode function $G''(\nu)$ corresponding to $n\to\infty$ is depicted in Fig. 2 by the solid curve with the amplitude $G''/G''_m=1$. It is seen from Fig. 2 how far the several tenth of the first successive approximations is from this limiting curve. So, the analysis of the approximate solutions of the integral equation (23) for the region of $k_c/\sqrt{\eta}\ll1$ by the method of the successive integration of the links of the infinite fraction Eq. (26) entails the cumbrous numerical calculations; the limiting transition to the case of the independent grains $k_c\to0$ is impossible by this method. At the same time, the region of small values of k_c is intensively investigated experimentally now[30] because it corresponds to the long correlations which appear in the real amorphous and nanocrystalline alloys for various physical reasons, inhomogeneities of the chemical composition, elastic stresses, and so on. But the main disadvantage of the method of the chain fraction is that permitting to investigate the region of the spin-wave resonances ($k\neq0$) this method does not permit to study the most important region of the magnetic susceptibility, the uniform ferromagnetic resonance. Equation (28) diverges and the imagination vanishes in Eq. (29) when the frequency ω approaches the FMR frequency ω_0 (and, correspondingly, the normalized frequency $\nu\to0$). As a result, Eq. (26) in the region of the FMR frequencies is inapplicable if we take into account any finite number of links of the chain fraction. That is why we propose here the another method of the analysis of the integral equation (23)—the method of algebraic equations. Contrary to the considered above method of chain fractions, the accuracy of the proposing method grows not with the increase but with the decrease of k_c. The main advantage of this method is that it permits us to investigate the whole frequency bond including the FMR.

B. Method of algebraic equations

Let us consider Eq. (23) at $k_c=0$. Then $S(\mathbf{k}-\mathbf{k}_1)=\delta(\mathbf{k}-\mathbf{k}_1)$, the integral in Eq. (23) can be performed exactly, and this equation transforms into an algebraic equation of the second power in $M_\mathbf{k}$ identical for 1D as well as 3D inhomogeneities. Retaining the only solution corresponding to $G''>0$ we obtain $M_\mathbf{k}$ from this equation in the form

$$M_k=\frac{1}{2}(\nu-k^2)+i\left[\eta^2-\frac{1}{4}(\nu-k^2)^2\right]^{1/2}. \tag{33}$$

The main assumption of the proposing method is that for obtaining the first approximation at $k_c\neq0$ we can set $M_{\mathbf{k}_1}\approx M_\mathbf{k}$ saving in the same time the spectral density $S(\mathbf{k}-\mathbf{k}_1)$ in the exact form. Under this assumption the integral in Eq. (23) is performed exactly and we obtain for the first approximation of $M_\mathbf{k}$ the following transcendental equations for the cases of the 1D and 3D inhomogeneities, respectively,

$$\text{1D,}\quad M_k=\frac{\eta^2}{(\sqrt{\nu-M_k}-ik_c)^2-k^2}\left(1-\frac{ik_c}{\sqrt{\nu-M_k}}\right), \tag{34}$$

$$\text{3D,}\quad M_k=\frac{\eta^2}{(\sqrt{\nu-M_k}-ik_c)^2-k^2}. \tag{35}$$

Pay attention that M_k depends only on a module of the vector $\mathbf{k}$ in both 1D and 3D cases.

Introducting the new variable $z=(\nu-M_k)^{1/2}$ we reduce these equations to the algebraic equations of the fifth and fourth power, respectively,

$$\text{1D,}\quad z(z^2-\nu)[(z-ik_c)^2-k^2]+\eta^2(z-ik_c)=0, \tag{36}$$

$$\text{3D,}\quad (z^2-\nu)[(z-ik_c)^2-k^2]+\eta^2=0. \tag{37}$$

The Green function has the form

$$\overline{G}=\frac{1}{z^2-k^2}. \tag{38}$$

Solutions of Eqs. (36) and (37) were found numerically. It turns out that not all roots of these equations satisfy the initial transcendental equations (34) and (35). That is why the following criterias are applied for the separation of the physical solution. First, the imaginary part of the mass term M_k must be positive from the physical reasons. Second, the solution of Eq. (36) or (37) must satisfy corresponding Eq. (34) or (35). These two criterias permit us uniquely to separate the physical resonance curve $G''(\nu,k)$.

The determined by this way continuous function $z(\nu,k)$, corresponding mass term $M_{\mathbf{k}}(\nu)$, and Green function $G_k(\nu)$ are the first approximation to the solution of the CPA equation (23). For obtaining the second approximation the mass term of the first approximation is substituted to Eq. (23) as a function of k_1. Performing the numerical integration in Eq. (23) we obtain M_k in the second approximation which can be substituted in the same equation again and so on, accordingly to the recurrent formula

$$M_k^{(n+1)} = \eta^2 \int \frac{S(\mathbf{k}-\mathbf{k}_1)d\mathbf{k}_1}{\nu - k_1^2 - M_{k_1}^{(n)}}. \tag{39}$$

The method of approximate solution of the integral CPA equation (23) that is proposed here, based on the reduction of this equation in the first approximation to the algebraic equation (36) or (37), has several advantages over the method of the numerical integration of the chain fraction (26). First, the function $G''(\nu,k)$ has no singularities at $k=0$ and it permits us for the first time to use the CPA method for investigating the FMR frequency band. Second, in the region of the large values of k, where both these methods are applicable, the method of the algebraic equations gives single-mode shape for the Green function even in the first approximation, whereas in the method of the chain fraction at small k_c the first approximation as well as a number of the following approximations leads to the physically senseless many-mode dependencies of $G''(\nu)$. Third, the method of the algebraic equations has a very quick convergence. Our studies show that even the first approximation is very good approximation of the exact result in the wide region of k_c and k. In the region of k_c and k where the first approximation is inadequate, the second or third approximation is usually good enough. Contrary to that, using the method of the chain fraction for the small k_c one must perform several tenths or even hundredths of successive integrations for obtaining the satisfactory result. And finally, the method of the algebraic equations permits us to obtain the approximate analytical expression for the Green function in some region of the parameters of the problem. At the conditions that $|M_k| \ll \nu, k^2$ the term M_k can be saved only in the resonance denominators of the equations of the first approximation; as a result, Eqs. (34) and (35) take the form, respectively,

$$\text{1D,} \quad M_k = \frac{\eta^2}{\nu - M_k - 2ik_c\sqrt{\nu} - k_c^2 - k^2} \frac{\sqrt{\nu} - ik_c}{\sqrt{\nu}}, \tag{40}$$

$$\text{3D,} \quad M_k = \frac{\eta^2}{\nu - M_k - 2ik_c\sqrt{\nu} - k_c^2 - k^2}. \tag{41}$$

Substituting solutions of these quadratic in M_k equations in Eq. (22) we obtain the explicit expressions for the Green function in the form

$$\text{1D,} \quad \overline{G} = \frac{1}{\nu - k^2 - P - i\left(\eta^2 \frac{\sqrt{\nu} - ik_c}{\sqrt{\nu}} - P^2\right)^{1/2}}, \tag{42}$$

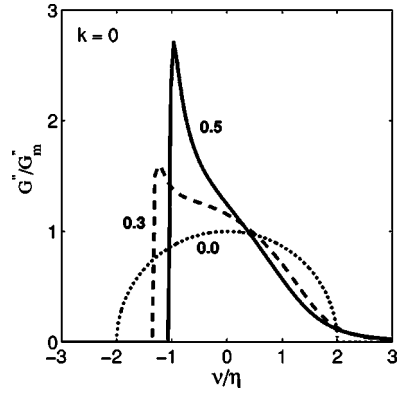

FIG. 3. The dependence of G'' at $k=0$ (FMR) on the normalized frequency ν/η for different values of the normalized correlation number of the 3D inhomogeneities $k_c/\sqrt{\eta}=0.0$, 0.3, and 0.5 which are shown near the corresponding curves.

$$\text{3D,} \quad \overline{G} = \frac{1}{\nu - k^2 - P - i(\eta^2 - P^2)^{1/2}}, \tag{43}$$

where

$$P = \frac{1}{2}[(\sqrt{\nu} - ik_c)^2 - k^2]. \tag{44}$$

IV. SHAPE AND WIDTH OF RESONANCE LINES

A. Ferromagnetic resonance

The shape of the resonance line is determined by the imaginary part of the averaged Green function $G''(\nu,k)$. At $k=0$ it describes the uniform resonance. The dependence G'' on ν at $k=0$ for the 3D inhomogeneities is shown in Fig. 3 for three values of the normalized correlation wave number $k_c/\sqrt{\eta}$ which are depicted near the corresponding curves. The dotted curve corresponds to the limiting case of the infinite correlation radius of the inhomogeneities ($k_c=0$, the independent grains limit). In this only case the integral equation of the CPA for M_k has the exact solution Eq. (33). Substituting this solution in Eq. (22) we obtain the following expressions for the real and imaginary parts of the Green function:

$$G' = \frac{1}{2\eta^2}\begin{cases} x, & x^2 \leqslant 4\eta^2, \\ x - \mathrm{sgn}(x)(x^2 - 4\eta^2)^{1/2}, & x^2 > 4\eta^2, \end{cases} \tag{45}$$

$$G'' = \frac{1}{2\eta^2}\begin{cases} (4\eta^2 - x^2)^{1/2}, & x^2 \leqslant 4\eta^2, \\ 0, & x^2 > 4\eta^2, \end{cases} \tag{46}$$

where $x=\nu-k^2$. These expressions do not depend on the dimensionality of the inhomogeneities. The approximate analytical equations (42) and (43) at $k_c=0$ also transform into exact ones and coincide between each other as well as with Eqs. (45) and (46). As is seen from Eq. (46) and Fig. 3 the function $G''(\nu)$ at $k_c=0$ vanishes for the values $\nu/\sqrt{\eta}$ outside the interval $(-2,+2)$ and reaches the maximum $G''/G''_m=1$ at $\nu=0$. The width of the resonance line in the half of its maximum is determined by the formula

$$\frac{\Delta\nu}{\eta} = \frac{\sqrt{5}\Delta H_0}{H_a} = 2\sqrt{3}, \tag{47}$$

This value is close to the result that has been obtained earlier[2,8] by the method of direct averaging for the model of independent grains: $\Delta H_0 \approx (5/3)H_a$.

When k_c becomes not equal zero (curves, corresponding to $k_c=0.3$ and 0.5 in Fig. 3) the physical mechanism of exchange narrowing of the FMR line switches on associated with averaging the local magnetic anisotropy over the volumes of the stochastic magnetic domains, the value of the resonance peak increases and its width decreases with the increase of k_c. In the same time at $k_c \neq 0$ the mechanism of broadening of the FMR line switches on associated with the damping induced by the scattering of the spin waves from the inhomogeneities. For the case of the FMR the latter mechanism leads to the asymmetry of the resonance line: the left edge of the line as before is characterized by the sharp rise, the decrease of the line becomes smooth. It is due to that the left part of the FMR line ($\nu<0$) is situated out of the limits of the spin-wave dispersion law $\nu=k^2$, while in the region $\nu>0$ at $k_c \neq 0$ the processes of the uniform precession decay into spin waves with $k \neq 0$ taking place which lead to broadening of the right part of the FMR line. However, the effects of exchange narrowing prevails in the total linewidth. The dependence of the FMR linewidth $\Delta\nu$ on the value of the correlation number k_c is shown in Fig. 4 for the 1D (crosses) and 3D (circles) inhomogeneities. For broadening the diapason of values of k_c the dependencies $\Delta\nu$ on $k_c/\sqrt{\eta}$ [Fig. 4(a)] as well as on the inverse value $\sqrt{\eta}/k_c$ [Fig. 4(b)] are shown in this figure. This is one of the main results of our work because it illustrates the effect of the FMR line exchange narrowing in the whole diapason of the correlation wave numbers k_c.

At $k_c=0$ the linewidth is maximum and determined by Eq. (47) when the anisotropy axis fluctuates and by the formula $\Delta H_0=2\sqrt{3}\gamma H_a$ when the anisotropy value fluctuates. Narrowing of the FMR line occurs with the increase of k_c and this effect develops itself for 3D inhomogeneities much stronger than for 1D inhomogeneities. For $k_c/\sqrt{\eta} \ll 1$ the line narrows linear in k_c. It follows from Fig. 4(a) that the dependencies ΔH on k_c in this region of k_c can be approximated by the formulas for 1D and 3D inhomogeneities, respectively,

$$\frac{\Delta H}{\Delta H_0} \approx \begin{cases} 1-0.45k_c/\sqrt{\eta}, & \text{1D}, \\ 1-1.1k_c/\sqrt{\eta}, & \text{3D}. \end{cases} \tag{48}$$

For the case of the anisotropy axis fluctuations we have $\eta=(\sqrt{5}L_0)^{1/2}$, $k_c=2/D_0$ and Eq. (48) can be written in the form

$$\frac{\Delta H}{\Delta H_0} \approx \begin{cases} 1-1.35L_0/D_0, & \text{1D}, \\ 1-3.3L_0/D_0, & \text{3D}. \end{cases} \tag{49}$$

In the opposite case of large values of k_c it appears that our numerical results are qualitatively described by Eqs. (1) and (2) which follow from the scaling arguments.[9] Comparing Eqs. (1) and (2) for $d=1$ and $d=3$ with the corresponding curves of Fig. 4(b) in the region of $\sqrt{\eta}/k_c \ll 1$ permits us to find the unknown constants a and b in Eq. (1) and to write

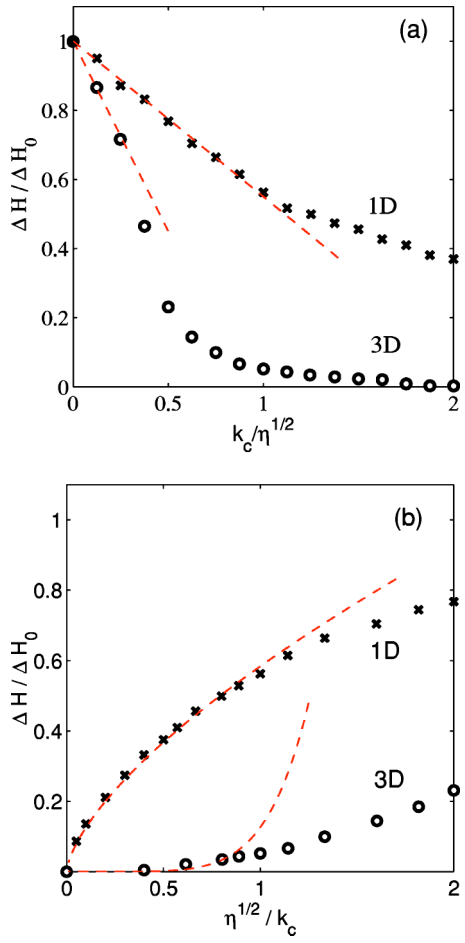

FIG. 4. The linewidth of the FMR ΔH as a function of the normalized correlation wave number $k_c/\sqrt{\eta}$ (a) and of the inverse value $\sqrt{\eta}/k_c$ (b) for the 1D (crosses) and 3D (circles) inhomogeneities. Dashed lines correspond to the approximate equations (48) (a) and (51) (b).

the formula for the FMR linewidth in this region in the form

$$\frac{\Delta H}{\Delta H_0} = \frac{1}{\sqrt{2}}\left(\frac{D_0}{4L_0}\right)^{2d(4-d)}, \tag{50}$$

or in our designations

$$\frac{\Delta H}{\Delta H_0} = \frac{1}{\sqrt{2}}\left(\frac{3\sqrt{\eta}}{4k_c}\right)^{2d(4-d)}. \tag{51}$$

The dependencies corresponding to Eq. (51) are shown in Fig. 4(b) by dashed curves for both dimensionalities $d=1$ and 3. So, it follows from the developed here theory as well as from the scaling arguments[9] that at $D_0 \ll L_0$ the FMR linewidth $\Delta H \propto D_0^{2/3}$ for the 1D and $\Delta H \propto D_0^6$ for the 3D inhomogeneities.

At $k_c \neq 0$ the shift of the resonance maximum takes place in the direction of the small frequencies, that are the negative values of ν (Fig. 5). This shift initially increases and then decreases with the k_c increase, going to zero with different rate for the 1D and 3D inhomogeneities. The maximum shift is in the vicinity of $k_c/\sqrt{\eta} \approx 0.7$ for the 1D and 0.25 for the

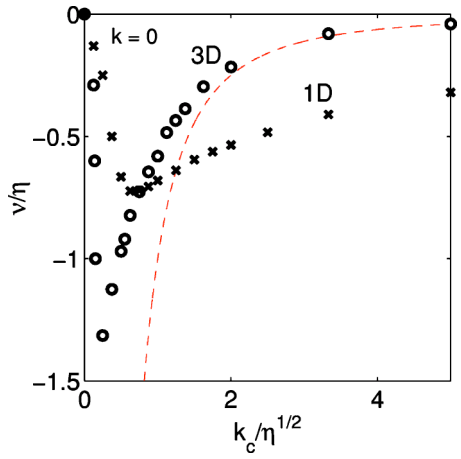

FIG. 5. The shift of the resonance maximum in dependence on the normalized correlation wave number $k_c/\sqrt{\eta}$ for 1D (crosses) and 3D (circles) inhomogeneities. The dashed curve shows the shift of the spin-wave eigenfrequency for $k=0$ calculated for the 3D inhomogeneities earlier (Ref. 15) in the framework of the perturbation theory.

3D inhomogeneities. The dependence of the FMR shift on k_c for the 3D inhomogeneities can be compared with the dependence of the spin-wave eigenfrequency on k_c which has been found earlier[15] by the perturbation theory methods,

$$\nu = k^2 - \frac{\eta^2}{k_c^2 + 4k^2}. \tag{52}$$

The latter dependence, that for the FMR has the form $\nu=-(\eta/k_c)^2$, is shown in Fig. 5 by the dashed curve. It is seen that for $k_c/\sqrt{\eta}\gg 1$ we have good agreement between the results of the perturbation theory and the CPA whereas for the small k_c the cardinal difference in the results takes place.

B. Spin waves

We consider oscillations with $k\neq 0$ now. The shape of the spin-wave resonance curve $G''(\nu)$ for the case of 3D inhomogeneities is shown in Fig. 6 at $k_c/\sqrt{\eta}=0.5$ for $k/\sqrt{\eta}=0.0$, 1.5, and 3.0. One can see that with the increase of k the function $G''(\nu)$ becomes more and more symmetric. It relates to that the spin-wave resonance, contrary to the FMR, takes place at the frequencies which lay inside the spin-wave band but not at the end of this band. Because of this the processes of the resonance precession decay into spin waves with another values of **k** go now in both the right and left edges of the resonance line. In Fig. 7 the dependencies of $\Delta\nu$ on k for the 1D (crosses) and 3D (circles) inhomogeneities are shown. For the comparison the dependence of the doubled value of the damping $2\nu''$ on k for the 3D case is shown in this figure by the dashed curve. The damping $\nu''(k)$ has been calculated earlier[15] by the perturbation theory and is determined by the formula

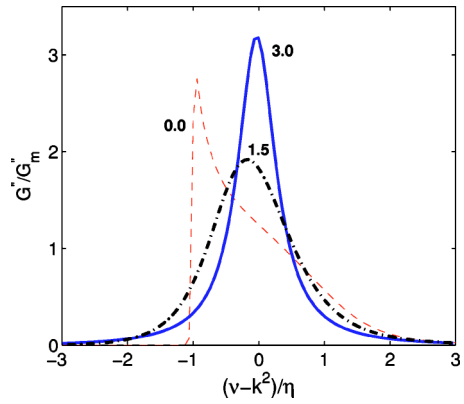

FIG. 6. The dependence G'' on the normalized frequency $(\nu-k^2)/\eta$ of the spin waves at $k_c/\sqrt{\eta}=0.5$ (3D case) for different values of the normalized waves number $k/\sqrt{\eta}=0.0$, 1.5, and 3.0 which are shown near the corresponding curves.

$$\nu'' = \frac{2\eta^2 k}{k_c(k_c^2 + 4k^2)}. \tag{53}$$

We note, that the same formula follows for ν'' in the first approximation in η^2 also from the equality to zero of the denominator of the approximate Green function Eq. (43).

It follows from Fig. 7 that in the region of the large k, corresponding to the inequality $k/\sqrt{\eta}\gg 1$, there is a good agreement between these values, $2\nu''\approx\Delta\nu$. However, there is a sharp difference between the function $\Delta\nu(k)$ and $2\nu''(k)$, both quantitative and qualitative, in the region of $k/\sqrt{\eta}<1$, the function $\nu''(k)$ decreases proportionally to k when $k\to 0$, the function $\Delta\nu(k)$ goes in this case to the finite FMR linewidth corresponding to the given k_c.

The latter illustrates the fact that the linewidth at small values of k is mainly determined by the stochastic distribution of the frequencies but not by the relaxation processes. It is also seen from Fig. 7 that the difference between the resonance linewidths for the cases of the 1D and 3D inhomogeneities is large at small k and decreases with the increase of k. At $k/\sqrt{\eta}\gg 1$ the linewidths for the 1D and 3D cases coin-

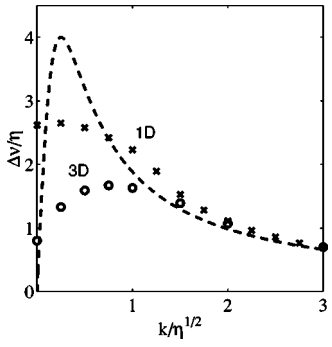

FIG. 7. The normalized linewidth of the spin waves $\Delta\nu/\eta$ as a function of the normalized wave number $k/\sqrt{\eta}$ for 1D (crosses) and 3D (circles) inhomogeneities with the correlation wave number $k_c/\sqrt{\eta}=0.5$. The dependence of the doubled value of the damping $2\nu''$ calculated for the 3D case earlier (Ref. 15) in the framework of the perturbation theory is shown by the dashed curve.

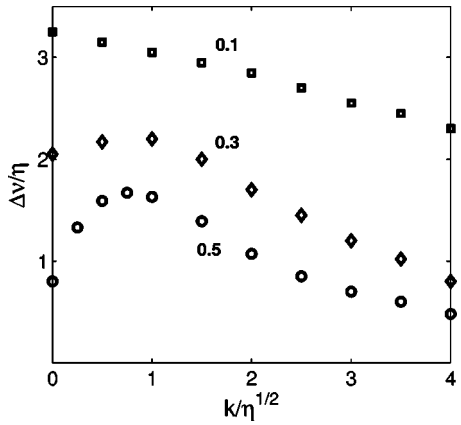

FIG. 8. The normalized linewidths of the spin waves $\Delta\nu/\eta$ for the 3D case as a function of the normalized wave number $k/\sqrt{\eta}$ for different values of $k_c/\sqrt{\eta}=0.1$, 0.3, and 0.5 which are shown near the corresponding curves.

cide between each other as well as with the doubled value of the damping $2\nu''(k)$.

In Fig. 8 the dependence of the spin-wave resonance linewidth on k is shown for the 3D inhomogeneities for different values of k_c. It is seen that the character of the functional dependence $\Delta\nu(k)$ changes with the increase of k_c. For the small k_c the linewidth decreases monotone with the increase of k. The maximum in the curve $\Delta\nu(k)$ appears in the vicinity of $k/\sqrt{\eta}\approx 1$ with the increase of k_c. For $k/\sqrt{\eta}\gg 1$ the each curve in Fig. 8 goes to the curve $2\nu''(k)$, corresponding to the given value of k_c. In Fig. 9 the dependence of the shift of the frequency of the resonance maximum ν on k is shown for the 1D (crosses) and 3D (circles) cases. The dependence of the eigenfrequency of the spin waves on k for the 3D case described by Eq. (52) is also shown (dashed curve). It is seen that all these three dependencies coincide at $k/\sqrt{\eta}\gg 1$ and diverge sharply at $k/\sqrt{\eta}\ll 1$.

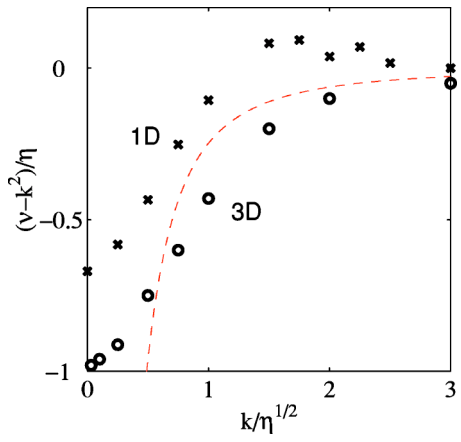

FIG. 9. The shift of the resonance maximum in the dependence on the normalized wave number $k/\sqrt{\eta}$ for 1D (crosses) and 3D (circles) inhomogeneities at $k_c/\sqrt{\eta}=0.5$. The dashed curve shows the dependence of the shift of the spin-wave eigenfrequency on the wave number $k/\sqrt{\eta}$ for the 3D case calculated in the framework of the perturbation theory (Ref. 15).

V. CONCLUSION

The shape and linewidth of the FMR and spin-wave resonances in a ferromagnet with the randomly inhomogeneous magnetic anisotropy is studied in this paper. The investigation is carried out by the method of Green functions in the framework of the coherent potential approximation. The method of the approximate solution of the CPA equation is proposed in which the first approximation is obtained as a result of the solution of the corresponding algebraic equation, the fifth and fourth powers for the 1D and 3D inhomogeneities, respectively. This method has several advantages over the usual, using for this aim the method of numerical integrating the corresponding chain fraction. The main advantage is that this method is applicable in the vicinity of the FMR resonance frequency $\nu=0$ where the method of the chain fraction leads to divergence of the corresponding integrals. It permits us to apply the CPA for investigation of exchange narrowing of the FMR line for the first time. This method has a very quick convergence, even first or second approximation is satisfactory in the wide region of the parameters of the system. The method has particular advantages for the small correlation wave numbers k_c (that is, for the large correlation radii of the inhomogeneities) because the first approximation turns to the exact solution of the CPA equation when $k_c\to 0$. Using this method we also manage to obtain approximate analytical expression for the Green function which is applicable in the wide region of the parameters excluding the vicinity of the FMR frequency $\nu=0$.

The dependencies of the width and shape of the resonance line as well as the shift of the resonance maximum on both the correlation wave number k_c and rms fluctuations η of the inhomogeneities are investigated for the FMR as well as the spin waves in a ferromagnet. The effects of exchange narrowing of the resonance line are obtained for the first time for the whole region of values of the correlation wave number k_c. For the FMR at $k_c=0$ the linewidth is maximum and corresponds to the limiting case of independent grains in the polycrystalline that have been considered earlier.[1,2] When $k_c>0$ the effect of exchange narrowing of the FMR line switches on associated with averaging the magnetic anisotropy as a consequence of the exchange coupling between the grains. Simultaneously the mechanism of broadening of the FMR line switches on associated with the scattering of spin waves from the inhomogeneities. The latter mechanism leads to the asymmetry of the resonance line. It is due to that the left part of the FMR line ($\nu<0$) is situated out of the limits of the spin-wave dispersion law $\nu=k^2$, while in the region $\nu>0$ the processes of the uniform precession decay into spin waves with $k\neq 0$ take place which lead to broadening of the right part of the FMR line. However, the effect of exchange narrowing prevails in the total linewidth. This effect develops itself for 3D inhomogeneities much stronger then for 1D ones. For the small k_c ($k_c\sqrt{\eta}\ll 1$) the linewidth decreases linear in k_c according to the asymptotic formulas (48) and (49) which have been obtained by approximation of the corresponding parts of the curves in Fig. 4(a). The change of the character of the dependence $\Delta H(k_c)$ occures in the vicinity of $k_c/\sqrt{\eta}\approx 1$. In the limiting case $k_c/\sqrt{\eta}\gg 1$ the

dependence $\Delta H/\Delta H_0$ on k_c is described qualitatively by Eqs. (1) and (2) which follow from the scaling arguments for the case of the strongly bounded grains.[9] It permits us to determine the unknown constants a and b in Eq. (1) (which appear to be independent on the dimensionality of inhomogeneities) and to write asymptotic formulas (50) and (51) for this limiting case. It follows from the experimental results[9] that ΔH changes approximately proportional to the change of the grain dimension D_0 in the process of annealing the sample. Such character of this dependency does not correspond to the expression either for the limiting case $\sqrt{\eta}/k_c \ll 1$ or for the limiting case $\sqrt{\eta}/k_c \gg 1$. However, it is seen from Fig. 4(b) that in the vicinity of $\sqrt{\eta}/k_c \approx 1$, where the character of the dependence $\Delta H(D_0)$ changes, the approximate proportionality between ΔH and D_0 can take place. The shift of the resonance maximum must occur also when k_c changes. The absolute value of this shift has a maximum in the vicinity of $k_c/\sqrt{\eta} \approx 0.25$ for the 3D case. For $k_c/\sqrt{\eta} \gg 1$ the shift of the FMR maximum coincides with the shift of the FMR eigenfrequency which has been calculated earlier by the perturbation theory.

The dependencies of the imaginary part of the Green function G'' on the frequency ν for the cases $k \neq 0$ which describe the susceptibilities of spin-wave resonances are also investigated in this paper. The effect of exchange narrowing of the resonance line with increase of k_c takes place in this case too. The asymmetry of the resonance line, which is characteristic for $k=0$, decreases with the increase of k because the spin-wave resonance at large k lays inside the spin-wave spectrum $\nu = k^2$, and the processes of the resonance precession decay take place at the both edges of the resonance line. The qualitative character of the dependencies $\Delta\nu(k_c)$ is the same for any k, but quantitative differences can be quite considerable. For the spin-wave resonance the dependencies the linewidth on k are of great interest which are depict in Fig. 8 for different k_c. It is shown that the character of these dependencies can be considerably different, the curves $\Delta\nu(k)$ can be monotonic or can have a maximum depending on the value of k_c. In the region of $k/\sqrt{\eta} \gg 1$ the dependence $\Delta\nu(k)$ coincides with the dependence of the doubled value of the damping $\nu''(k)$ which has been calculated earlier by the perturbation theory methods; in the same time there is the sharp difference between $\Delta\nu(k)$ and $2\nu''(k)$ in the region of $k/\sqrt{\eta} \ll 1$. The analogous picture is observed also when comparing the dependencies of the resonance maximum shifts and eigenfrequencies on k.

The effects of exchange narrowing of the FMR as well as spin-wave resonance lines connect between each other the main structural characteristics of the inhomogeneities (k_c and η) with the main applied characteristics of the matter, that are the magnetic resonance linewidths. Large narrowing of the FMR and spin-wave linewidths with the decrease of the correlation radius of inhomogeneities obtained in this paper is the substantiation of the main advantage of the nanocrystalline and amorphous materials over usual polycrystals when they are used at high frequency devices.

ACKNOWLEDGMENTS

This work was supported by the Russian Foundation for Basic Researches, Grant No. 04-04-16174 and the Krasnoyarsk Regional Science Foundation, Grant No. 12F0013C.

[1] E. Schlomann, J. Phys. Chem. Solids **6**, 257 (1958).
[2] E. Schlomann and J. R. Zeender, J. Appl. Phys. **29**, 341 (1958).
[3] A. G. Gurevich, *Magnetic Resonance in Ferrites and Antiferromagnetics* (Nauka, Moscow, 1973).
[4] R. Kubo and K. J. Tomita, J. Phys. Soc. Jpn. **9**, 888 (1954); R. Kubo, *ibid.* **9**, 935 (1954).
[5] A. Abragam, *The Principles of Nuclear Magnetism* (Clarendon, Oxford, 1961).
[6] S. A. Altshuler and B. M. Kozyrev, *Electronic Paramagnetic Resonance of Compounds of Elements of Intermediate Groups* (Nauka, Moscow, 1972).
[7] S. Geschwind and A. M. Clogston, Phys. Rev. **108**, 49 (1957).
[8] D. L. Griscom, J. Non-Cryst. Solids **67**, 81 (1981).
[9] M. Rubistein, V. G. Harris, and P. Lubitz, J. Magn. Magn. Mater. **234**, 306 (2001).
[10] R. Alben, J. J. Becker, and M. C. Chi, J. Appl. Phys. **49**, 1653 (1978).
[11] G. Herzer, IEEE Trans. Magn. **25**, 3327 (1989).
[12] R. S. Iskhakov, S. V. Komogortsev, A. D. Balaev, and L. A. Chekanova, Pis'ma Zh. Eksp. Teor. Fiz. **72**, 440 (2000) [JETP Lett. **72**, 304 (2000)].
[13] R. Skomski, J. Phys.: Condens. Matter **15**, R841 (2003).
[14] E. C. Stoner and E. P. Wohlfart, Philos. Trans. R. Soc. London, Ser. A **240**, 599 (1948).
[15] V. A. Ignatchenko and R. S. Iskhakov, Zh. Eksp. Teor. Fiz. **72**, 1005 (1977) [Sov. Phys. JETP **45**, 526 (1977)].
[16] I. Ya. Korenblit and E. F. Shender, J. Phys. F: Met. Phys. **9**, 2245 (1979).
[17] M. V. Medvedev and M. V. Sadovsky, Fiz. Tverd. Tela (Leningrad) **23**, 1943 (1981).
[18] K. Handrich and R. Öttking, Phys. Status Solidi B **216**, 1073 (1999).
[19] V. A. Ignatchenko, Zh. Eksp. Teor. Fiz. **54**, 303 (1968).
[20] S. M. Rytov, Yu. A. Kravtsov, and V. I. Tatarsky, *Introduction to Statistical Radiophysics (part II: Random Fields)* (Nauka, Moscow, 1978).
[21] E. N. Economou, *Green's Functions in Quantum Physics* (Springer-Verlag, Berlin, 1982).
[22] I. M. Lifshits, S. A. Gredeskul, and L. A. Pastur, *Introduction to the Theory of Disorder Systems* (Nauka, Moscow, 1982).
[23] J. M. Ziman, *Models of Disorder* (Cambridge University Press, Cambridge, 1979).
[24] P. Soven, Phys. Rev. **156**, 809 (1967).
[25] D. W. Taylor, Phys. Rev. **156**, 1017 (1967).
[26] B. Velický, S. Kirkpatrick, and H. Ehrenreich, Phys. Rev. **175**, 747 (1968).
[27] G. Brown, V. Celli, M. Haller, A. Maradudin, and A. Marvin,

Phys. Rev. B **31**, 4993 (1985).
[28] R. J. Elliott, J. A. Krumhansl, and P. L. Leath, Rev. Mod. Phys. **46**, 465 (1974).
[29] R. C. Bourret, Nuovo Cimento **26**, 1 (1962); Can. J. Phys. **40**, 783 (1962).
[30] V. A. Ignatchenko and R. S. Iskhakov, in *Magnetic Properties of Crystalline and Amorphous Mediums*, edited by V. A. Ignatchenko (Nauka, Novosibirsk, 1989).